| Ber. nat.-med. Ver. Salzburg | Band 15 | S. 109-117 | Salzburg 2008 |
|---|---|---|---|

# ANALYSIS AND MODELLING OF THE *SELSONICS* ULTRASONIC NEBULIZATION CHAMBER

## ANALYSE UND MODELLIERUNG DER *SELSONICS* ULTRASCHALL ZERSTÄUBER KAMMER

PIERRE MADL*, WERNER HOFMANN

**Abstract**

Vitamin-C enriched sodium-chloride (15% NaCl solution) from the Dead Sea and organically grown and extracted olive-oil samples with traces of supplemented Vitamin-D (totalling 5mL each) were separately nebulized by ultrasound atomizers in a therapeutic aerosol chamber specifically design and constructed for this purpose by Selsonics GmbH. Particle growth dynamics from aerosol processing reactions were measured with a Scanning Mobility Particle Sizer (SMPS) immediately after a 3 minutes long sample injection sequence. Scanning times with the SMPS covered a potential exposure window of at least 9 minutes in the size range of 0.01 to 1.1 µm. Based on the data obtained from the SMPS measurements, the stochastic lung particle deposition model IDEAL, latest version (KOBLINGER & HOFMANN 1990, HOFMANN & KOBLINGER 1990) was to compute and the associated particle deposition patterns.

**Keywords**: therapeutic aerosol chamber, sodium-chloride particles, olive-oil particles, inhalation, lung deposition, size distribution.

**Zusammenfassung**

Proben von mit Vitamin-C angereichertes Natrium-Chlorid (15% NaCl Lösung) aus dem Toten Meer und mit Vitamin-D angereichertes Olivenöl aus biologischem Anbau (jeweils a 5mL) wurden einzeln und durch separate Ultraschall-Vernebler in einer extra zu diesem Zweck entwickelten und gebauten therapeutischen Expositionskammer der Firma Selsonics GmbH zerstäubt. Nach einer 3 Minuten dauernden Injektionsphase in die Kammer wurde die Wachstumsdynamik des Aerosols mithelfe eines abtastenden Mobilitäts Messer (SMPS) erfasst. Die Abtastdauer umfasste ein typische Expositiondauer von mindestens 9 Minuten und erfolgte in einem Grössenklassen-Bereich zwischen 01 to 1.1 µm. Basierend auf die



biophysics.sbg.ac.at/home.htm

dabei erhaltenen Messdaten wurde das stochastische Lungen-Depositionsmodell IDEAL in der letzten Version (KOBLINGER & HOFMANN 1990; HOFMANN & KOBLINGER 1990) angewandt um Partikel-Depositionen in den jeweiligen Lugnenbereichen zu modellieren.

**Schlüsselwörter**: therapeutische Aerosol-Kammer, Salz-Partikel, Olivenöl-Partikel, Inhalation, Lungendeposition, Grössenverteilung.

## Introduction

Aerosol inhalation using Selsonic's exposure chamber is achieved via two separate ultrasound nebulizers. Two vials containing 5mL each - one filled with vitamin-C enriched saltwater from the Dead Sea, the other with vitamin-D enriched virgin olive oil (DAB-standards) - are placed into separate drawers (see Fig. 1). Once the vials are in place, an automated procedure operates the nebulization routine, starting with a 5 minute long salt-exposure (of which 3 minutes constitute the actual nebulization window), followed by an identical sequence in which the oil is vaporized. In-between the samples as well as at the end and of the exposure, the chamber is flushed via two powerful ventilation fans.


**Figure 1:** Selsonic nebulization chamber. The nebulizer on the top left (1) emits NaCl aerosol, whereas the one on the top right (2) is used for olive-oil vaporization. The drawers for the vials (3) house the monousable NaCl- and oil vials respectively (image: Selsonics, 2007)

## Methods

This enclosed exposure study was done in a therapeutical chamber designed and made by Selsonics GmbH, located in Ampfing, Germany. Nebulization of both 5 mL liquid salt and oil samples was carried out by atomizers using ultrasound technology. Measurements of the nebulized samples were made with the SMPS model (Grimm Aerosol Technik). This mobile continuous nano-particle counter combines a Condensation Nucleus Counter (model #5.403) and a Direct Mobility Analyzer „Vienna-Type“, (model #5.500), using an L-DMA suitable to detect a size range from 10 to 1100 nm.

The observed particle spectra of the oil- and NaCl-samples are documented in Fig. 2. The oil-spectrum reveals a polydisperse distribution with the geometric mean located at around 140 nm. Particle concentrations peaked at around $103 \cdot 10^3 \pm 26 \cdot 10^3$ particles$\cdot$cm$^{-3}$ and gradually decreased afterwards as agglomeration to larger clusters took place. In the same figure, the observed particle spectrum of the NaCl-sample is incorporated. Here, the geometric mean was located at around 240 nm, while particle concentrations peaked at around $30 \cdot 10^3 \pm 4.8 \cdot 10^3$ particles$\cdot$cm$^{-3}$ and gradually decreased afterwards due to agglomeration to larger clusters.

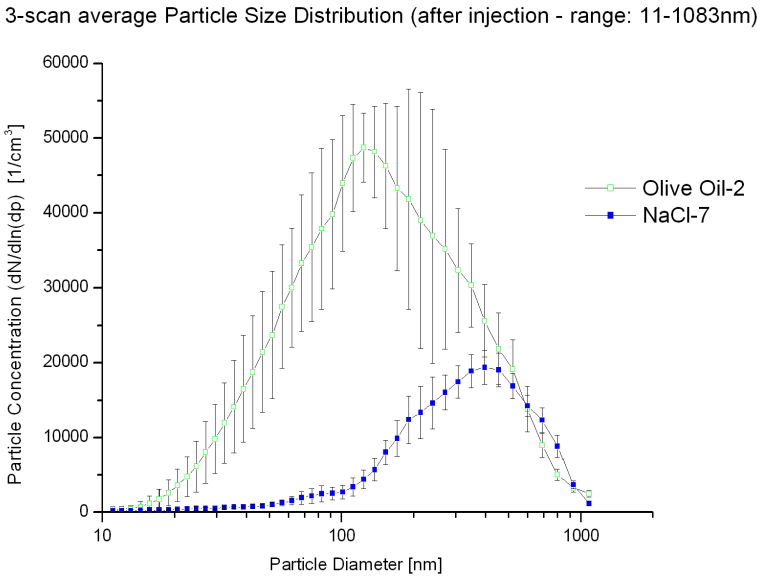


**Figure 2:** Size class particle distribution of an olive-oil- and NaCl aerosol over a time window of 9 minutes. Average total particle concentration of olive oil was found at $103 \cdot 10^3 \pm 26 \cdot 10^3 \cdot$cm$^{-3}$ and that of NaCl at $30 \cdot 10^3 \pm 4.8 \cdot 10^3 \cdot$cm$^{-3}$.

To investigate the fate of inhaled particles, we applied the stochastic lung model developed by KOBLINGER and HOFMANN (1990) to model deposition over the size range of 10 to 1100 nm using the 44 output channels of the SMPS – each channel corresponds to a specific size class with a corresponding number particle concentration. The corresponding data - pairs of number concentration and size class - were used to run the latest version of the stochastic lung particle deposition model IDEAL (KOBLINGER & HOFMANN 1990; HOFMANN & KOBLINGER 1990). In this model the geometry of the airways along the path of an inhaled particle is selected randomly using a Monte Carlo code IDEAL, whereas deposition probabilities are computed by deterministic formulae. In addition, the airway geometry selection, the random walk of particles through this geometry and the methods of aerosol deposition calculation in conductive and respiratory airways during a full breathing cycle are incorporated in this model. Altogether, the model enables computation of total, regional and differential particle deposition in a stochastic lung structure.

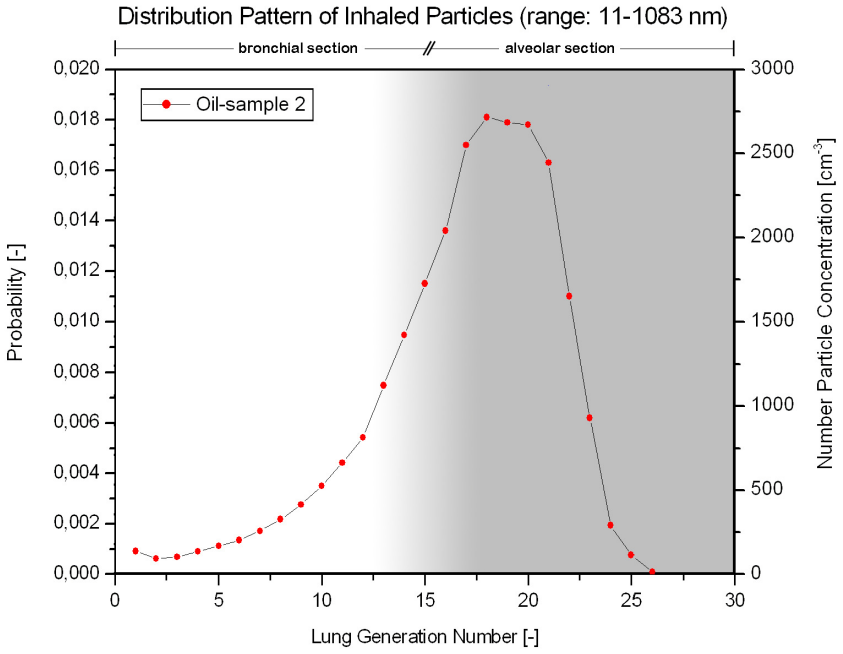


**Figure 3a:** Modelled distribution of the olive-oil aerosol deposition within the respiratory tract over 27 generations. Extrathoracic deposition 8.93% - total lung deposition: 26.5%.

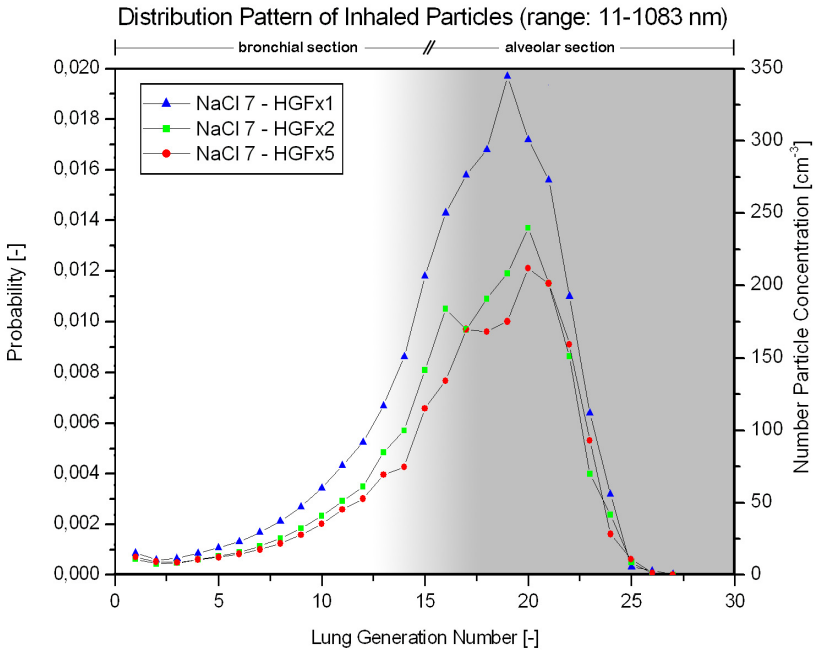


**Figure 3b:** Modelled distribution of NaCl-aerosol deposition within the respiratory tract.

HGFx1: extrathoracic deposition: 8.99% - total lung deposition: 26.2%.
HGFx2: extrathoracic deposition: 6.55% - total lung deposition: 18.5%.
HGFx5: extrathoracic deposition: 7.53% - total lung deposition: 18.3%.

The above figures 3.a & b reveal the potential deposition patterns of the samples within the human lung. The frequency on the left ordinate is plotted as a dimensionless parameter, thus given in percent when multiplied by a conversion factor of 100. The right ordinate refers to the same set of data and presents the absolute number particle concentrations with respect to each generation. Generation-numbers plotted on the abscissa correspond to the various pulmonary regions, with the trachea being generation 0, while generation 1 to 15 are associated to the bronchial region. The regimes above are related to the alveolar regime (YEH & SCHUM 1980). It was assumed that particle morphology corresponds to a spherical shape with a unit particle density of $\rho = 1$ g/cm$^3$.

## Results

Particle deposition of the nebulized oil sample outlines the deep-reaching pulmonary properties of this aerosol. Due to the minute size of the particle load along with the hydrophobic attribute of this sample, bronchial deposition is negligible, whereas alveolar deposition predominates. Particle deposition of the nebulized NaCl sample follows a similar distribution pattern. However, a proportionally larger fraction is deposited within the tracheo-bronchial regime. With relative humidity levels in the human respiratory tract equalling almost 100 %, the hydrophilic character of this sample results in additional deposition within the bronchial regime (see fig. 3.b - HGFx5). Considering this elevated humidity level within the pulmonary region, the scan with the hygroscopic growth factor (HGF) of 5 can be assigned to the hydrophilic NaCl aerosol and approximates real-world conditions (HEYDER et al. 2004). However, an intermediate HGF of 2 was likewise modelled to illustrate the altered deposition properties with increasing particle growth.
According to the human lung model published by YEH and SCHUM (1980) inhaled particle deposition is spread across the tracheo-bronchial and the alveolar-acinar regions. Since there is no sharp threshold between these two regions in a realistic lung structure, for simplicity YEH and SCHUM (1980) separated these two regions by assigning those above the $15^{th}$ generation alveolar status whereas those below belong to the bronchial region. Based on these assumptions, we conclude that the alveolar deposition, especially from hydrophobic particles such as nebulized olive oil tend to increasingly deposit in higher generation airways (alveolar regime), and to a lesser extent into within the bronchial region where ciliary motion would translocate deposited particles promptly via the mucociliary clearance. Hence, alveolar deposition is associated with an increased imuno-response activity by alveolar macrophages (DONALDSON et al. 1998).

## Discussion

Inhalation of particles is widely used in medical therapy as well as in the wellness sector, yet so far the methodology involved here differs substantially from those used in conventional applications. Using nano-sized particles greatly enhances the penetration efficiency to evoke various responses of the human body. As observed in Fig. 3 a-b, the size range of the inhaled particles easily reaches the alveolar region well beyond the $15^{th}$ lung generation. Alveolar congestion by the inhaled particle load can largely be excluded, as the detected nano-particles are some $1 \cdot 10^3$ to $10 \cdot 10^3$ times smaller than the tiniest alveolar duct-diameters (BURRI 1985). As shown in Fig. 2, the potentially huge bolus concentration of the olive oil spectrum, amounting to approx. $103 \cdot 10^3$ particles$\cdot$cm$^{-3}$ is spread over 27 lung generations further dividing the overall concentration by an approximated factor of $2^{27}$. Hence, even extremely large concentrations of inhaled particles do not support agglomeration and obstructive effects within the alveolar regime. Considering particle kinetics after aerosol injection within the chamber along with the volume of air to be inhaled, one

can expect a slightly elevated inhaled particle load as the SMPS sampled the chamber by a continuous flow of 0.3 L/min only. That is, a relaxed person inside the chamber would have a tidal respiratory volume of about 0.5 L along with roughly 12 in-/exhalations per minute, which yields a total of 6 L of inhaled respiratory air. In relation to the 0.3 L/min of the sampling device, this corresponds to a 20-fold increase of the inhaled particle load. Since total scanning windows of the SMPS lasted 9 minutes for each nebulized sample and the fact that a person would just be exposed to 5 minutes per sample each – with flushing cycles in-between – the actual proportionality factor would just be $5/9^{th}$ of 20, thus estimated to be around 11-times that of the detected SMPS-concentrations (compare fig.2). Figures 3 a-b clearly highlight the partial deposition efficiency modeled with the measured data. In the case of olive oil inhalation about 26.5% and in the case of sodium chloride between about 18.3 % are deposited within the entire respiratory tract – which includes the extrathoracic deposition. These values seem sufficient to induce a stimulating effect on the entire organism (MULZ, 2007). Due to super-saturated conditions within the human lung only the NaCl-graph highlighting the HGFx5 distribution pattern should be taken into consideration (HEYDER et al. 2004).

Environmental tobacco smoke (ETS) for example differs drastically in composition and in chemical reactivity. ETS is largely constituted of partially burnt substances, with an average number of over 4000 different highly reactive chemicals (KHAN, 2006). Furthermore, fresh cigarette smoke is found to have a count mean diameter of 210 nm and a concentration of $2.86 \cdot 10^9$ particles/cm$^3$ (ROBINSON & YU, 2001). Thus, not only the amount but also the type of a cigarette aerosol radically differs from aerosol inhalation of unaltered and pristine substances like olive oil and sodium chloride. On the contrary such aerosol particles are thought to have a positive effect on human health as inhalation of such aerosols aids in the dislodgement of excess mucus from bronchi (DAVISKAS et al. 1996).

Nebulization of hydrophilic and hydrophobic substances is not only limited to inhalation per se, whole body dermal exposure is another issue to consider. Perspiration is the production and passive evaporation of bodily fluid, consisting primarily of water via the active transport of tiny amount of minerals - among them sodium chloride - excreted by the sweat glands in the skin. Thus direct dermal exposure of salt-aerosols rapidly re-establishes a balanced cellular mineral homeostasis. Already previous investigation utilized olive oil and aqueous aerosols in exposure experiments (TSUDA et al. 1984). However, this research group employed droplet sizes that were well beyond 1 µm in diameter. Hence dermal and inhalatory absorption of aerosols exceeding average cell sizes is impaired, whereas nano-sized aerosols can be considered as being ideal size classes for rapid phagocytic and selective uptake by the exposed cells (MULZ 2007).

It has been demonstrated that sniffing nano-sized aerosols not only easily pass the blood-brain barrier via humoral transport, but they are also readily absorbed via skin and mucous membranes (BUCHBAUER 2003). According to LEVINE et al. (2000) the skin can be considered as the body's largest organ (approx. 2 m$^2$), percutane

absorption efficiency is just third after intestinal adsorption (approx. 300 $m^2$) and lung inhalation (approx. 150 $m^2$ surface area in adults). Both percutane absorption and inhalation of nano-sized aerosols get rid of the so-called first-pass effect (FPE) – that is the biological transformation and, in some cases, elimination of a substance in the liver after absorption from the intestine and before it reaches systemic circulation (GOLD & SEHMI 2004). Elimination of the FPE would enable exposure to considerably lower dosage of the substances involved and as a result could significantly reduce potential side effects.
As outlined by the potential application in treating respiratory ailments from people experiencing increased respiratory airflow resistance (DAVISKAS et al. 1996), ANGEROSA (1995) highlighted the aroma-therapeutic aspect of virgin olive oil inhalation to stimulate the proteic receptors and neurons of the olfactory system. Moreover, the vast number of $C_6$-volatiles, aldehydes, alcohols and esters are directly routed into the cells without being subject to the FPE. GOLDFRANK et al. (2002) emphasized the decontaminant properties of olive oils in dermal application, as it absorbs toxic substances like phenols and prevent their further absorption. In addition, the authors state that cutaneous decontamination decreased systemic effects and facilitated healing of dermal burns. Hence it may not come as a surprise that whole-body aerosol exposure of other ethereal oils and/or watery solutions along with aerosol inhalation may proof far more efficient than conventional inhalation therapy using a mouth-piece only. This chamber could evoke interest in rehabilitation and reconstituting applications, but also in medical studies investigating therapeutical effects in the treatment of *Actelectasis* – a condition where the alveoli are deflated, in people suffering from hay-fever, neurodermitis (*Atopic dermatitis*), psoriasis, etc. and even in post-scar treatment smoothening hardened dermal scar-tissue (MULZ 2007). The 5 mL required could prove sufficient to achieve respiratory relief in people with cardiovascular and respiratory difficulties (DAVISKAS et al. 1996, MULZ 2007).

**Acknowledgements**

The authors wish to thank to the people from Selsonics for their kind assistance, in particular to P. Huber technical officer at Selsonics and to Mr. P. Richter, managing director of Selsonics GmbH. http://www.selsonics.com/Selsonics_E/produkt_e.html

**References**

ANGEROSA F. (1995): Sensory Qualities of olive Oils; : Analysis and Properties; In: HARWOOD J.L., APARICIO R., HARWOOD J. (eds.). -The Handbook of Olive Oil; Springer Verlag: 1-360

BUCHBAUER G. (2003): Biologische Wirkungen von Ätherischen Ölen und Duftstoffen; 2003. Plenarvortrag am 33ten Internationalen Symposium über Ätherische Öle (ISEO) in Lissabon, - ÖAZ 14: 76

BURRI P. H. (1985): Morphology and Respiratory Function of the Alveolar Unit. - International Archives of Allergy and Applied Immunology,76.

DAVISKAS E., ANDERSON S. D., GONDA I., EBERL S., MEIKLE S., SEALE J. P., BAUTOVICH G. (1996): Inhalation of hypertonic saline aerosol enhances mucociliary clearance in asthmatic and healthy subjects; - European Respiratory Journal; 9: 725–73

DONALDSON K., LI X. Y., MACNEE W. (1998): Ultrafine (Nanometre) Particle Mediated Lung Injury. - Journal of Aerosol Science, 29, Issues 5-6

GOLD V., SEHMI P. (2004): Compendium of Chemical Terminology. International Union of Pure and Applied Chemistry (IUPAC), 76: 1052

GOLDFRANK L. R., FLOMENBAUM N., LEWIN N., HOWLAND M. A., HOFFMAN R., NELSON L. (2002): Antiseptics, Desinfectants and Sterilants; In: GOLDFRANK L. R. (ed).; Goldfrank's Toxicologic Emergencies, 7th ed.; MacGraw-Hill; Ch.84: 1283

HEYDER J., GEBHART J, ROTH C., FERRON G. (2004): Transport and deposition of hydrophilic drug particles in the lungs. In: GRADON L., MARIJNISSEN, J.C. (eds.).; Optimization of Aerosol Drug Delivery; - Springer Verlag, Heidelberg: 139-147

HOFMANN W, KOBLINGER L. (1990): Monte Carlo modeling of aerosol deposition in human lungs. Part II: Deposition fractions and their sensitivity to parameter variations. - Journal of Aerosol Science, 21: 675-688

KHAN M. I. G., (2006): Encyclopedia of Heart Diseases. ; Effects of Smoking in Heart disease. - Academic Press; Ch.55: 335

KOBLINGER L., HOFMANN W. (1990): Monte Carlo modeling of aerosol deposition in human lungs. Part I: Simulation of particle transport in a stochastic lungs structure. - Journal of Aerosol Science. 21: 661-674

LEVINE R. R., WALSH C. T., SCHWARTZ-BLOOM R. D. (2000): Pharmacology: Drug Actions and Reactions, 6th ed. Taylor & Francis Group

MULZ D. O. (2007): Personal communication by Prof. Dr.Dr.D.O.MULZ at the Selsonic's Workshop on the 22nd / 23rd Feb. 2007 held in Ampfing, FRG

ROBINSON R. J., YU C. P. (2001): Deposition of Cigarette Smoke Particles in the Human Respiratory Tract. - Aerosol Science and Technology, 34: 202–215

TSUDA S., IWASAKIM., YOSHIDA M., SHIRASU Y. (1984): Inhalation Chamber with Size Discriminator for Liquid Aerosols. - Toxicological Sciences, 4: 378-387

YEH H. C., SCHUM G.M. (1980): Models of human lung airways and their application to inhaled particle deposition. - Bull Math Biol ; 42: 461-480

**Anschriften der Verfasser:**

Division of Physics and Biophysics
Department of Materials Engineering & Physics
Paris Lodron University of Salzburg (PLUS),
Hellbrunner Str. 34, A-5020 Salzburg, Austria